

Degradation induced decrease of the radiative quantum efficiency in organic light-emitting diodes

Cite as: Appl. Phys. Lett. **101**, 103301 (2012); <https://doi.org/10.1063/1.4749815>

Submitted: 04 July 2012 . Accepted: 20 August 2012 . Published Online: 04 September 2012

Tobias D. Schmidt, Daniel S. Setz, Michael Flämmich, Bert J. Scholz, Arndt Jaeger, Carola Diez, Dirk Michaelis, Norbert Danz, and Wolfgang Brütting



View Online



Export Citation

ARTICLES YOU MAY BE INTERESTED IN

[Analyzing degradation effects of organic light-emitting diodes via transient optical and electrical measurements](#)

Journal of Applied Physics **117**, 215502 (2015); <https://doi.org/10.1063/1.4921829>

[Intrinsic luminance loss in phosphorescent small-molecule organic light emitting devices due to bimolecular annihilation reactions](#)

Journal of Applied Physics **103**, 044509 (2008); <https://doi.org/10.1063/1.2884530>

[Impedance spectroscopy as a probe for the degradation of organic light-emitting diodes](#)

Journal of Applied Physics **107**, 054501 (2010); <https://doi.org/10.1063/1.3294642>

Lock-in Amplifiers

... and more, from DC to 600 MHz



Degradation induced decrease of the radiative quantum efficiency in organic light-emitting diodes

Tobias D. Schmidt,^{1,a)} Daniel S. Setz,² Michael Flämmich,³ Bert J. Scholz,¹ Arndt Jaeger,² Carola Diez,² Dirk Michaelis,³ Norbert Danz,³ and Wolfgang Brütting^{1,b)}

¹*Institute of Physics, University of Augsburg, 86135 Augsburg, Germany*

²*OSRAM Opto Semiconductors GmbH, Leibnizstrasse 4, 93055 Regensburg, Germany*

³*Fraunhofer Institute for Applied Optics and Precision Engineering, 07745 Jena, Germany*

(Received 4 July 2012; accepted 20 August 2012; published online 4 September 2012)

The efficiency decrease during electrical operation of organic light-emitting diodes is a crucial issue for both applied and fundamental research. In order to investigate degradation processes, we have performed an efficiency analysis for phosphorescent state-of-the-art devices in the pristine state and after an accelerated aging process at high current density resulting in a luminance drop to less than 60% of the initial value. This loss in efficiency can be explained by a decrease of the radiative quantum efficiency of the light-emitting guest/host system from 70% to 40%, while other factors determining the efficiency are not affected. © 2012 American Institute of Physics. [<http://dx.doi.org/10.1063/1.4749815>]

Organic light-emitting diodes (OLEDs) are promising light sources for applications in general lighting and displays. In recent years the external quantum efficiency (EQE) of the devices has grown continuously, especially since phosphorescent emitters with high intrinsic radiative quantum efficiencies (RQEs) have been applied to OLEDs.^{1–3} Commercial applications such as white OLED lamps have already been introduced to the market by several companies with long lifetimes exceeding 5000 h. Nevertheless, further improvements of lifetime and efficiency will pave the way for broad usage of OLED lighting products in the future. In this paper we present a method that allows one to quantify the influence of degradation on the different factors of the external quantum efficiency of OLEDs.

The EQE of an OLED is given by⁴

$$\text{EQE} = \gamma \cdot \eta_{s/t} \cdot q_{\text{eff}}(q) \cdot \eta_{\text{out}}, \quad (1)$$

where γ is the charge carrier balance and $\eta_{s/t}$ represents the fraction of excitons that is allowed to decay radiatively by quantum mechanical selection rules. q_{eff} is the effective RQE of the emitter material,⁵ which depends on the intrinsic radiative quantum efficiency (q) modified by the Purcell effect, if the emitter is embedded in a microcavity-like structure, as in an OLED. Finally, η_{out} is the light outcoupling factor, which is mainly determined by the optical environment, i.e., the refractive indices and thicknesses of the layers used in the device, and the orientation of the light-emitting molecules.^{6,7}

A comprehensive efficiency analysis has been performed to analyze degradation effects during electrical operation. The method is based on a variation of the electron transport layer (ETL) thickness resulting in different emitter/cathode distances corresponding to different lengths of the optical cavity. Consequently, excited state lifetimes are

changed by the so-called Purcell effect⁸ that enables one to determine the RQE (i.e., q) of the phosphorescent guest-host system used. Additionally, the prevailing emitter orientation, resulting outcoupling factors, and charge carrier balance can be investigated. Performing time-resolved optical spectroscopy and EQE measurements on electrically driven OLEDs and comparing these findings with numerical simulations including possible deviations from random emitter orientation allow for a determination of both the charge carrier balance of the device and the RQE of the emitting system.^{6,7,9,10}

We have analyzed a set of phosphorescent state-of-the-art OLEDs employing the red emitting molecule Iridium(III)bis(2-methylbenzo-[f,h]quinoxaline)(acetylacetonate) (Ir(MDQ)₂(acac)) doped with 8 wt. % in an N,N'-bis(naphthalen-1-yl)-N,N'-bis(phenyl)benzidine (α -NPD) matrix as emitting guest/host system. OLED stack and chemical structures of the molecules are shown in Fig. 1. It is known from previous publications that this emitting system exhibits predominantly horizontal oriented emissive dipole moments, which has to be considered for efficiency analysis to achieve consistent results.^{6,10} Nine OLEDs with different ETL thicknesses and an active area of 4 mm² have been fabricated to allow for a systematic efficiency analysis before and after degradation. For details of device fabrication we refer to a previously published article.¹⁰ All electrically driven EQE measurements have been performed in a calibrated integrating sphere at a low current density j of 1 mA/cm² to minimize quenching effects like triplet-triplet-annihilation (TTA) or triplet-polaron-quenching (TPQ).^{9,11} Time-resolved optical spectroscopy was performed by exciting the emission layer inside the OLED structure with a short nitrogen laser pulse (wavelength 337 nm, pulse energy 10 μ J, pulse duration 750 ps; MNL-202 C Laser Technik Berlin) and analyzing simultaneously the decay signal both temporally and wavelength-dependently (SpectraPro 2300i, Princeton Instruments) with a commercial streak-camera system from Hamamatsu Photonics (C5680). This allows for a signal separation of the

^{a)}Electronic mail: Tobias.Schmidt@physik.uni-augsburg.de.

^{b)}Electronic mail: Wolfgang.Brueetting@physik.uni-augsburg.de.

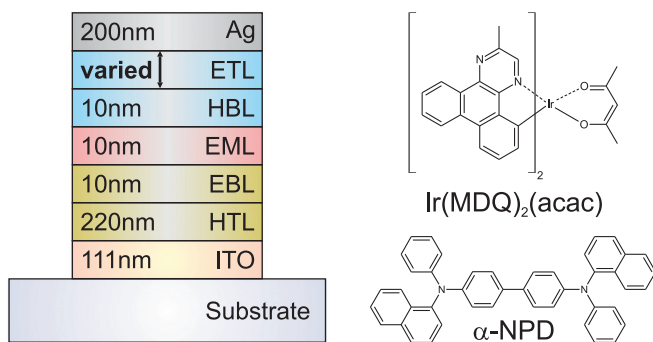


FIG. 1. Device stack and chemical structures of the emitting guest/host system.

emission layer, e.g., excited transport and blocking layers. The decay curves have been analyzed by integrating over the whole spectrum of the emitter material from 550 nm to 750 nm. Strictly speaking, the ETL variation changes the length of the cavity which in turn influences both the emission spectrum and the lifetime of excitons emitting at different wavelengths. However, since our simulation for calculating the Purcell factor is based on an integration over the whole emission spectrum, the same method should be applied for the analysis of the experimental data to be consistent.

The aging of these devices was accomplished by electrical operation at high current densities and therefore high brightnesses. These high current densities correspond to accelerated testing conditions in OLED applications. Applying a constant current density of 62.5 mA/cm^2 to each of the OLEDs for nearly 70 hours results in a significant drop of the measured luminance, but only a slight increase of the required voltage.¹² Figure 2 shows an exemplary current-voltage-luminance (I-V-L) characteristic and the degradation curve of a device having an ETL thickness of 249 nm. The drop of the luminance to less than 60% of the initial value is reached after 65 h stress time. The stretched exponential luminance decrease with aging time is representative for deactivation of emissive centers during the degradation process.¹³ Nevertheless, only small changes of the

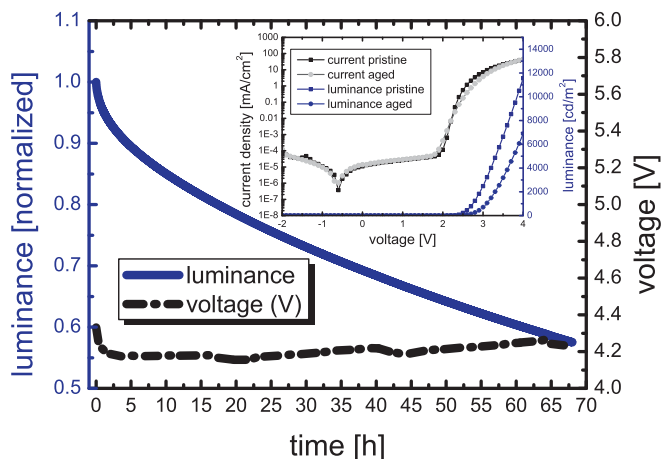


FIG. 2. Accelerated degradation curve (blue, solid line: luminance; black, dashed line: voltage) for a constant driving current density of 62.5 mA/cm^2 resulting in an initial luminance of about 15000 cd/m^2 for the red OLED stack with 249 nm ETL thickness. The inset shows the I-V-L characteristics of the device in the pristine state and after degradation.

electrical behavior are detectable, as can be seen from the inset of Fig. 2.

Although the ETL thicknesses of the devices are varying, resulting in completely different positions of the emissive layer in the microcavity formed by the metallic cathode and the semi-transparent anode, the degradation behavior is very similar as can be seen from the compilation in Fig. 3. To analyze this behavior, EQE measurements of electrically driven OLEDs at a current density of 1 mA/cm^2 have been performed for all devices before and after aging. All nine devices show comparable relative changes of their EQE, although the absolute values differ considerably for the various ETL thicknesses. This systematic decrease of the EQE is the basis for an efficiency analysis after degradation as presented for the pristine stack in Ref. 6. The lines in Fig. 3 show best fits based on optical simulations for the determination of the radiative quantum efficiency of the emitting system, yielding q values of $(68 \pm 2) \%$ in the pristine state and of $(40 \pm 2) \%$ after degradation, respectively. Note that all simulations have been performed for the present predominantly horizontal emitter orientation ratio of 2:0.63 parallel to vertical (with respect to the surface of the OLED) oriented emissive dipole moments. Note that in the isotropic case one would have an orientation ratio of 2:1, while a completely horizontal orientation would lead to a ratio of 2:0. For more information on the determination of the emitter orientation and the orientation factor we refer to Refs. 6 and 10. The decrease of the radiative quantum efficiency of the emitting system by 41% can fully explain the luminance drop after accelerated aging and gives evidence that this is the dominant mechanism for device degradation in this study.

Another outcome of the simulations is that the charge carrier balance has not changed during electrical operation and remains constant ($\gamma \approx 1$) due to appropriate blocking and doped transport layers. This can be seen by the good agreement of measurement and simulation, which was performed for an ideal charge carrier balance. As pointed out in Ref. 9, smaller values of γ cannot simply be compensated by

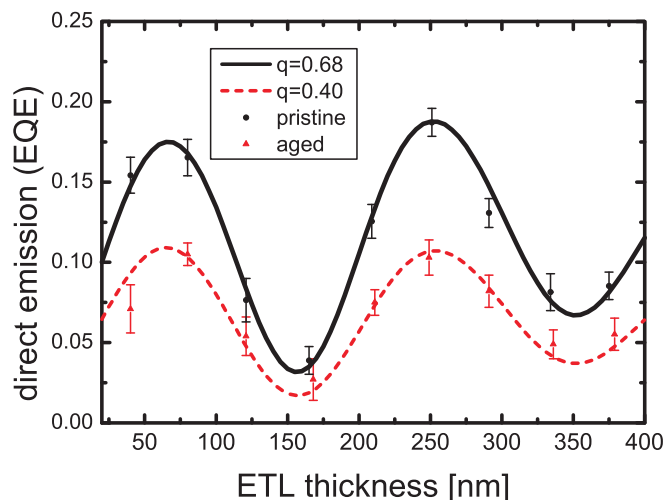


FIG. 3. Determination of the radiative quantum efficiency of the investigated emitting system in the pristine state (black dots) and after the degradation process (red triangles) using external quantum efficiency measurements at a current density of 1 mA/cm^2 . The lines are optical simulations for different intrinsic radiative quantum efficiencies (black line: $q = 0.68$; red line: $q = 0.40$).

using a larger RQE value in the simulation as this would lead to a different relative height of the interference maxima in the EQE. To ensure that degradation does not affect the outcoupling factor, we followed the route¹⁴ to prove similar emitter orientation and emission zone for both pristine and degraded devices. Therefore, we are confident that electrical operation does not influence the outcoupling factor of these devices (see Eq. (1)).

Time-resolved optical spectroscopy has been performed in order to better understand the degradation induced decrease of the RQE of the phosphorescent emitting system. The intrinsic excited states lifetime (τ_0) is given by the inverse sum of the radiative (k_r) and the non-radiative (k_{nr}) decay rates (in the absence of a cavity)

$$\tau_0 = (k_r + k_{nr})^{-1}. \quad (2)$$

Based on that, the intrinsic radiative quantum efficiency (q) of an emitting system is defined as the product of the radiative rate and the excited states lifetime

$$q = k_r \cdot \tau_0 = \frac{k_r}{k_r + k_{nr}}. \quad (3)$$

As mentioned at the beginning of the article, the excited states lifetime and the RQE are modified by the Purcell effect, if the emitting system is embedded in a microcavity. Thus the radiative rate has to be multiplied by the Purcell factor F resulting in a modified excited states lifetime (τ) and an effective radiative quantum efficiency (q_{eff}) given by the following equations¹⁵

$$\tau = (F \cdot k_r + k_{nr})^{-1}, \quad (4)$$

$$q_{\text{eff}} = F \cdot k_r \cdot \tau = \frac{F \cdot k_r}{F \cdot k_r + k_{nr}}. \quad (5)$$

It is to be expected that the excited states lifetime (τ) for all samples with varying position of the emissive layer in the microcavity decreases after electrical operation, as a result of an increase of the non-radiative rate (k_{nr}).^{16,17} Figure 4 shows an exemplary mono-exponential photoluminescence decay curve for the pristine state and after degradation for an ETL thickness of 168 nm. The measured phosphorescence lifetime for the device with an ETL thickness near the first cavity minimum drops from 1.55 μs to 1.30 μs due to the electrical degradation. Figure 5 shows the measured phosphorescence lifetimes for the pristine state and after degradation together with best fits of simulated lifetime changes for the varying ETL thicknesses. These fits are based on a least square error procedure with q and τ_0 as fitting parameters. This method yields a q of $(70 \pm 5)\%$ for the pristine devices with an intrinsic excited states lifetime τ_0 of $(1.37 \pm 0.03)\ \mu\text{s}$. For the aged devices the RQE (termed now q^* for clarity) drops to $(40 \pm 5)\%$ with a modified τ_0^* of $(1.23 \pm 0.03)\ \mu\text{s}$. The RQEs determined in this way are in good agreement with the values obtained from EQE measurements. This confirms the hypothesis that the luminance drop during electrical aging is mainly a consequence of a decreasing radiative quantum efficiency of the guest/host system used for the devices under study.

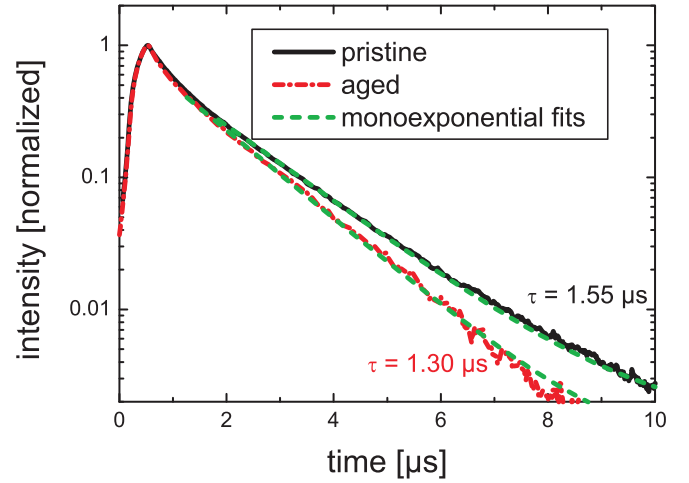


FIG. 4. Time-resolved photoluminescence measurements for the pristine state (black, solid line) and after the degradation (red, dashed line) of the OLED with an ETL thickness of 168 nm. Green dashed lines show mono-exponential fits with an additional offset due to a constant background signal for both curves. The excited states lifetime gets reduced by the degradation process.

Moreover, it is possible to calculate the intrinsic radiative and non-radiative decay rates from these time-resolved optical measurements for the pristine emitting system and after degradation. Solving Eqs. (2) and (3) with the determined q and τ_0 results in values of $k_r = 5.1 \cdot 10^5\ \text{s}^{-1}$ and $k_{nr} = 2.2 \cdot 10^5\ \text{s}^{-1}$ for the pristine devices. In the same way from τ_0^* and q^* after degradation one obtains a radiative decay rate k_r^* of $3.3 \cdot 10^5\ \text{s}^{-1}$ and a non-radiative decay rate k_{nr}^* of $4.8 \cdot 10^5\ \text{s}^{-1}$. As expected from other experiments^{16,17} the non-radiative rate increases due to the aging. However, it is evident that also the radiative rate is modified and decreases upon device degradation.

Thus the straightforward assumption of an unchanged radiative rate is wrong. This implies that not only the emitter but also the matrix material α -NPD, and hence the surrounding media of the emitting dye molecules, is affected due to electrical aging. Therefore, we assume two possible effects

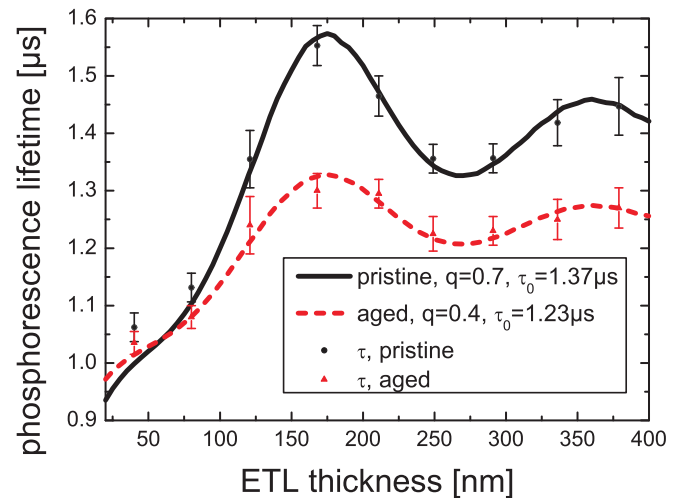


FIG. 5. Determination of the radiative quantum efficiency of the used emitting system for the pristine state (black dots) and after the degradation process (red triangles) via changes of the excited states lifetime. The colored lines are optical simulations for different radiative quantum efficiencies and intrinsic lifetimes.

to explain the changes of both the radiative and the non-radiative rate, namely, a degradation of the host as well as a degradation of the phosphorescent guest molecules.

With regard to matrix effects, it is known that α -NPD is not stable under current flow and reacts chemically with its surroundings, creating non-radiative recombination centers and charge carrier traps.^{12,18–20} One possible effect is that the electronic levels of these degradation products are shifted in energy with respect to the pristine molecules, which can influence the Dexter transfer rate (k_D) from the host to the phosphorescent guest. If the energy transfer rate to Ir(MDQ)₂ (acac) is drastically reduced due to degradation of the α -NPD molecules and the decay rates of the emitting species is of the same magnitude as the degraded transfer rate k_D^* , one would expect a bi-exponential decay behavior of the measured phosphorescence with an initial slow increase of the signal. As can be seen from Fig. 4 this is actually not the case. Therefore, we assume two other effects that can explain the changes in the non-radiative and the radiative decay rate of the emitting molecules. As mentioned before, the non-radiative decay rate of the emitting molecules can be enhanced by both the degraded matrix molecules themselves, acting as emission quenchers, and charge carriers that are trapped on the matrix can be responsible for triplet-polaron-quenching. In addition, the degraded matrix molecules can exhibit a different permittivity with respect to their intact counterparts. This could explain the changed radiative decay rate of the embedded dye molecules due to changes in the optical environment.

Besides matrix effects the emitter molecule Ir(MDQ)₂ (acac) can react chemically under replacement of its ligands. These products (deactivated sites) are normally not able to emit light. This behavior is known for many Ir-complexes such as Ir(ppy)₃ or Ir(ppy)₂(acac),²¹ which have similar structures as Ir(MDQ)₂(acac),²² and from devices using Alq₃ as emitting system.²³ Energy transfer from the host as well as from intact emitting molecules to these degradation products can increase the non-radiative decay rate and reduce the Dexter transfer rate by opening up a competing transfer channel or by simply depleting the guest/host system from intact dye molecules. In addition, the degradation of emitters might lead to rather subtle molecular changes only. In that case, one could expect a similar emission spectrum of these degradation products exhibiting different decay times. This could be another reason for the changed radiative and non-radiative decay rates.

In conclusion, we have analyzed degradation effects in state-of-the-art organic light-emitting diodes. Our approach

allows us to quantify the influence of electrical changes and the decrease of the radiative quantum efficiency of the phosphorescent guest/host system on the luminance drop during electrical aging. Furthermore, time-resolved phosphorescence measurements reveal that both emitter and matrix show degradation effects which decrease the efficiency of the devices. In addition we have investigated the emitter orientation for the pristine state and after degradation but could not detect any changes due to electrical operation.

We acknowledge financial support by the German Federal Ministry of Education and Research (BMBF) under the Contract No. FKZ 13N10474 (TOPAS 2012).

- ¹M. A. Baldo, D. F. O'Brien, Y. You, A. Shoustikov, S. Silbey, M. E. Thompson, and S. R. Forrest, *Nature (London)* **395**, 151 (1998).
- ²C. Adachi, M. A. Baldo, M. E. Thompson, and S. R. Forrest, *J. Appl. Phys.* **90**, 5048 (2001).
- ³S. Reineke, F. Lindner, G. Schwartz, N. Seidler, K. Walzer, B. Lüssem, and K. Leo, *Nature (London)* **459**, 234–238 (2009).
- ⁴T. Tsutsui, E. Aminaka, C. P. Lin, and D.-U. Kim, *Trans. R. Soc. London, Ser. A* **355**, 801–814 (1997).
- ⁵S. Nowy, B. C. Krummacher, J. Frischeisen, N. Reinke, and W. Brütting, *J. Appl. Phys.* **104**, 123109 (2008).
- ⁶T. D. Schmidt, D. S. Setz, M. Flämmich, J. Frischeisen, D. Michaelis, B. C. Krummacher, N. Danz, and W. Brütting, *Appl. Phys. Lett.* **99**, 163302 (2011).
- ⁷T. D. Schmidt, M. Flämmich, B. J. Scholz, D. Michaelis, C. Mayr, N. Danz, and W. Brütting, *Proc. SPIE* **8435**, 843513 (2012).
- ⁸E. M. Purcell, *Phys. Rev.* **69**, 674 (1946).
- ⁹D. S. Setz, T. D. Schmidt, M. Flämmich, S. Nowy, J. Frischeisen, B. C. Krummacher, T. Dobbertin, K. Heuser, D. Michaelis, N. Danz, W. Brütting, and A. Winnacker, *J. Photon. Energy* **1**, 011006 (2011).
- ¹⁰M. Flämmich, J. Frischeisen, D. S. Setz, D. Michaelis, B. C. Krummacher, T. D. Schmidt, W. Brütting, and N. Danz, *Org. Electron.* **12**, 1663 (2011).
- ¹¹N. C. Giebink and S. R. Forrest, *Phys. Rev. B* **77**, 235215 (2008).
- ¹²F. So and D. Y. Kondakov, *Adv. Mater.* **22**, 3762–3777 (2010).
- ¹³C. Fery, B. Racine, D. Vaufrey, H. Doyeux, and S. Cina, *Appl. Phys. Lett.* **87**, 213502 (2005).
- ¹⁴M. Flämmich, D. Michaelis, and N. Danz, *Org. Electron.* **12**, 83–91 (2011).
- ¹⁵S. Mladenovski, S. Reineke, and K. Neyts, *Opt. Lett.* **34**, 1375 (2009).
- ¹⁶Z. D. Popovic, H. Aziz, A. Ioannidis, N.-X. Hu, and P. N. M. dos Anjos, *Synth. Met.* **123**, 179–181 (2001).
- ¹⁷Z. D. Popovic, H. Aziz, A. Ioannidis, N.-X. Hu, and P. N. M. dos Anjos, *J. Appl. Phys.* **89**, 4673–4675 (2001).
- ¹⁸D. Y. Kondakov and R. H. Young, *J. Appl. Phys.* **108**, 074513 (2010).
- ¹⁹D. Y. Kondakov, *J. Appl. Phys.* **104**, 084520 (2008).
- ²⁰N. C. Giebink, B. W. D'Andrade, M. S. Weaver, J. J. Brown, and S. R. Forrest, *J. Appl. Phys.* **105**, 124514 (2009).
- ²¹I. R. de Moraes, S. Scholz, B. Lüssem, and K. Leo, *Appl. Phys. Lett.* **99**, 053302 (2011).
- ²²R. Meerheim, S. Scholz, S. Olthof, G. Schwartz, S. Reineke, K. Walzer, and K. Leo, *J. Appl. Phys.* **104**, 014510 (2008).
- ²³S. Scholz, B. Lüssem, and K. Leo, *Appl. Phys. Lett.* **95**, 183309 (2009).